Inhibitory effect of black tea pigments, theaflavin-3/3'-gallate against cisplatin-resistant ovarian cancer cells by inducing apoptosis and G1 cell cycle arrest

HAIBO PAN[1,2], FANG WANG[3], GARY O. RANKIN[4], YON ROJANASAKUL[5], YOUYING TU[1] and YI CHARLIE CHEN[2]

[1]Department of Tea Science, Zhejiang University, Hangzhou, Zhejiang, P.R. China; [2]College of Science, Technology and Mathematics, Alderson Broaddus University, Philippi, WV, USA; [3]Department of Tea Science, Wuyi University, Wuyishan, Fujian, P.R. China; [4]Department of Biomedical Sciences, Joan C. Edwards School of Medicine, Marshall University, Huntington; [5]Department of Pharmaceutical Sciences, West Virginia University, Morgantown, WV, USA

Abstract. Adverse side effects and acquired resistance to conventional chemotherapy based on platinum drive the exploration of other selective anticancer drugs. Theaflavin-3-gallate (TF2a) and theaflavin-3'-gallate (TF2b), theaflavin monomers in black tea, exhibited a potent growth inhibitory effect on cisplatin-resistant ovarian cancer A2780/CP70 cells and were less cytotoxic to normal ovarian IOSE-364 cell line. Flow cytometry analysis and western blotting indicated that TF2a and TF2b induced apoptosis and G1 cell cycle arrest in ovarian cancer A2780/CP70 cells. Hoechst 33342 staining was used to confirm the apoptotic effect. Downregulation of CDK2 and CDK4 for TF2a and CDK2 and cyclin E1 for TF2b led to the accumulation of cells in G1 phase. TF2a and TF2b induced apoptosis and G1 through p53-dependent pathways. TF2a and TF2b induced DNA damage through ATM/Chk/p53 pathway. TF2a and TF2b also induced inhibition of A2780/CP70 cells through Akt and MAPK pathways. The results of this study implied that TF2a and TF2b might help prevent and treat platinum-resistant ovarian cancer.

Introduction

Ovarian cancer ranks fifth in cancer deaths among women in the United States, accounting for ~5% of all cancer deaths diagnosed among women (1). Among the gynecologic cancers (uterine, cervical and ovarian), ovarian cancer has the highest rate of deaths. The conventional course of therapy is maximal surgical resection of the tumor mass, followed by chemotherapy based on taxane and platinum (2). Despite 70% of patients responding well to first-line platinum-based therapy, the emergence of side effects and drug resistance has rendered a variety of the currently available chemotherapeutic drugs ineffective (3). The 5-year survival rate for patients with advanced ovarian cancer remains <40% because of acquired drug resistance and adverse side effects (4,5). Hence, there is an urgent need to explore novel therapeutic interventions and overcome drug resistance for this disease.

Natural products have played a beneficial role in cancer treatment for >50 years (6-8). They have already afforded some clinically used chemotherapeutic agents, and are a proven resource to explore new anticancer drugs for further cancer research. Thus, out of 175 small-molecule chemotherapy drugs in Western countries over a period of ~70 years, ~49% were either obtained from organisms directly or derived from natural products (8).

Black tea is one of the most widely consumed beverages around the world. A prospective cohort study showed that black tea consumption appeared to be inversely correlated with some cancer risks induced by smoking and a reduced intake of vegetables and fruits (9). In particular, US women mainly ingested dietary flavonols from black tea, and flavonol intake could lower the risk of ovarian cancer (10). Theaflavins are the major bioactive components in black tea. They are orange or orange-red in color and possess a benzotropolone skeleton that is formed from the co-oxidation of selected pairs of catechins during black tea production (11). The major theaflavins in black tea are theaflavin (TF1), theaflavin-3-gallate (TF2a), theaflavin-3'-gallate (TF2b) and theaflavin-3,3'-digallate (TF3). Theaflavins have been demonstrated to inhibit lung tumorigenesis in A/J mice (12) and a variety of cancer cells including SV40 transformed WI38 human cells (13), Caco-2 colon cancer cells (13), human stomach

Correspondence to: Dr Yi Charlie Chen, College of Science, Technology and Mathematics, Alderson Broaddus University, 101 College Hill Drive, Philippi, WV 26416, USA
E-mail: chenyc@ab.edu

Dr Youying Tu, Department of Tea Science, Zhejiang University, 866 Yuhangtang Road, Hangzhou, Zhejiang 310058, P.R. China
E-mail: youytu@zju.edu.cn

cancer Kato III cells (14) and human breast cancer cells (15). We have previously reported that TF3 could induce apoptosis and cell cycle arrest (16) and inhibit angiogenesis (17) in human ovarian carcinoma cells. TF2a and TF2b showed similar inhibitory effect on human ovarian carcinoma cells to TF3 (18), but their effect against ovarian cancer is not yet clear. Therefore, we aimed to investigate the inhibitory effect of TF2a and TF2b on the platinum-resistant ovarian cancer cell line A2780/CP70 and a normal ovarian surface epithelial IOSE-364 cell line. The possible mechanisms by which TF2a and TF2b-induced apoptosis and cell cycle arrest and the detailed molecular signaling pathway in the ovarian cancer cells were explored.

Materials and methods

Cell culture and reagents. The platinum-resistant human ovarian cancer cell line A2780/CP70 (p53 wild-type) was presented by Dr Binghua Jiang at West Virginia University. The normal ovarian surface epithelial cell line, IOSE-364 was a gift from Dr Nelly Auersperg at University of British Columbia. The cells were cultured in RPMI-1640 medium (Sigma, St. Louis, MO, USA) supplemented with 10% fetal bovine serum (FBS) (Invitrogen, Rockford, IL, USA) at 37°C in a humidified incubator with 5% CO_2. TF2a and TF2b monomers were isolated and purified using a previous method (19). Primary antibodies to caspase-3, cleaved caspase-3 (Asp175), caspase-7, cleaved caspase-7 (Asp198), cyclin D1, cyclin E1 (D7T3U), CDK2 (78B2), CDK4 (D9G3E), p21$^{Waf1/Cip1}$ (12D1), p53 (7F5), ATM (D2E2), p-ATM (Ser1981 (D6H9), histone H2AX (Dl7A3), p-histone H2AX (Ser139), Akt, p-Akt (Ser473), p38, p-p38 (Thr180/Tyr182) (28B10), JNK and JNK (Thr183/Tyr185) were purchased from Cell Signaling Inc. (Danvers, MA, USA). Primary antibodies PARP-1 (F-2), chk1 (G4), p-chk1 (Ser345), chk2 (H-300), p-chk2 (Thr68), p-p53 (Ser15), ERK1 (K-23), p-ERK1/2 (Thr202), GAPDH (0411) and the secondary antibodies were purchased from Santa Cruz Biotechnology Inc. (Mariposa, CA, USA).

Cell viability assay. The cell viability was assessed using [3-(4,5-dimethylthiazol-2-yl)-5- (3-carboxymethoxyphenyl)-2-(4-sulfophenyl)-2H-tetrazolium (MTS) assay. A2780/CP70 cells were seeded into 96-well plates at a density of $2x10^4$ cells per well and incubated overnight. Then cells were treated with different concentrations of TF2a and TF2b (0-40 μM) or an equal amount of dimethyl sulfoxide (DMSO) (as vehicle) (Sigma) for 24 h. Cell viability was measured using CellTiter 96® Aqueous One Solution Cell Proliferation assay kit (Promega, St. Louis, MO, USA), according to the manufacturer's instructions. Cell viability was expressed as a percentage compared to that of control cells (vehicle treatment).

LDH cytotoxicity assay. A2780/CP70 cells were seeded in 96-well plates with the density of $2x10^4$ cells per well and incubated overnight. Then cells were treated with different concentrations of TF2a and TF2b (0-40 μM) or an equal amount of DMSO (as vehicle) for 24 h. After incubation, LDH was determined by LDH cytotoxicity assay kit (Thermo Fisher Scientific, Waltham, MA, USA) according to the manufacturer's instructions.

Hoechst 33342 staining. A2780/CP70 cells were seeded in 24-well plates at $2x10^4$ cells/well and incubated overnight. Cells were treated with TF2a and TF2b (0, 5, 10 and 20 μM) for 24 h. Then the cells were stained with 10 μg/ml Hoechst 33342 (Sigma) in PBS for 10 min in the dark at 37°C. Cellular morphology was examined under a fluorescence microscope (ZEISS).

Flow cytometric analysis of apoptotic cells. Cell apoptosis was determined using an Alexa Fluor® 488 Annexin V/ Dead Cell Apoptosis kit (Invitrogen). After treatment with TF2a and TF2b (0, 5, 10 and 20 μM) for 24 h, A2780/CP70 cells were collected, centrifuged for 10 min at 1,500 rpm and then washed twice with PBS. Cells were stained in binding buffer with Alexa Fluor 488 Annexin V and propidium iodide (PI) for 15 min. The stained cells were determined with flow cytometry (FACSCalibur system; BD Biosciences), measuring the fluorescence emission at 530 and 575 nm using 488 nm excitation.

Flow cytometry analysis of the cell cycle. A2780/CP70 cells treated with TF2a and TF2b (0, 5, 10 and 20 μM) for 24 h were collected, suspended in 70% ethanol and stored at -20°C overnight. Then the cells were washed twice with PBS and incubated with 180 μg/ml RNase A (Invitrogen) at 37°C for 15 min. After 15 min staining with 50 μg/ml PI (Sigma) in the dark at 37°C, the cells were analyzed by flow cytometry (FACSCalibur system; BD Biosciences).

Caspase-3/7 assay. A2780/CP70 cells were seeded in 96-well plates at the density of $2x10^4$ cells per well, incubated overnight. Then the cells were treated with TF2a and TF2b (0, 5, 10 and 20 μM) for 24 h. After 24-h treatment, 100 μl of caspase-3/7 reagent was added to each well, mixed well and incubated for 1 h at 37°C. The caspase-3/7 activities in cells were determined using a Caspase-Glo 3/7 assay kit (Promega) according to the manufacturer's instructions. A Synergy™ HT Multi-Mode Microplate Reader (BioTek) was used to measure luminescence. Total protein levels were used to normalize the caspase-3/7 activities. The caspase-3/7 activities were expressed as a percentage compared to that of the untreated control. A BCA assay kit (Pierce, St. Louis, MO, USA) was used to measure total protein levels in the cells.

Western blotting. A2780/CP70 cells were seeded in 60-mm dishes at the density of $1x10^6$ cells/dish, incubated overnight, and treated with TF2a and TF2b (0, 5, 10 and 20 μM) for 24 h. Then the cells were collected with M-PER Mammalian Protein Extraction Reagent (Pierce) supplemented with Halt™ Protease and Phosphatase Inhibitor Single-Use Cocktail (Life Technologies, Grand Island, NY, USA). The total protein levels were detected with BCA Protein assay kit (Pierce). Equal amounts of protein were separated by sodium dodecyl sulfate polyacrylamide gel electrophoresis and transferred onto nitrocellulose membranes. The membrane was blocked with 5% skim milk in Tris-buffer saline containing 0.1% Tween-20 for 1 h at room temperature, and then incubated with specific primary antibodies and appropriate secondary antibodies conjugated with horseradish peroxidase. The antigen-antibody complex was visualized with Super Signal
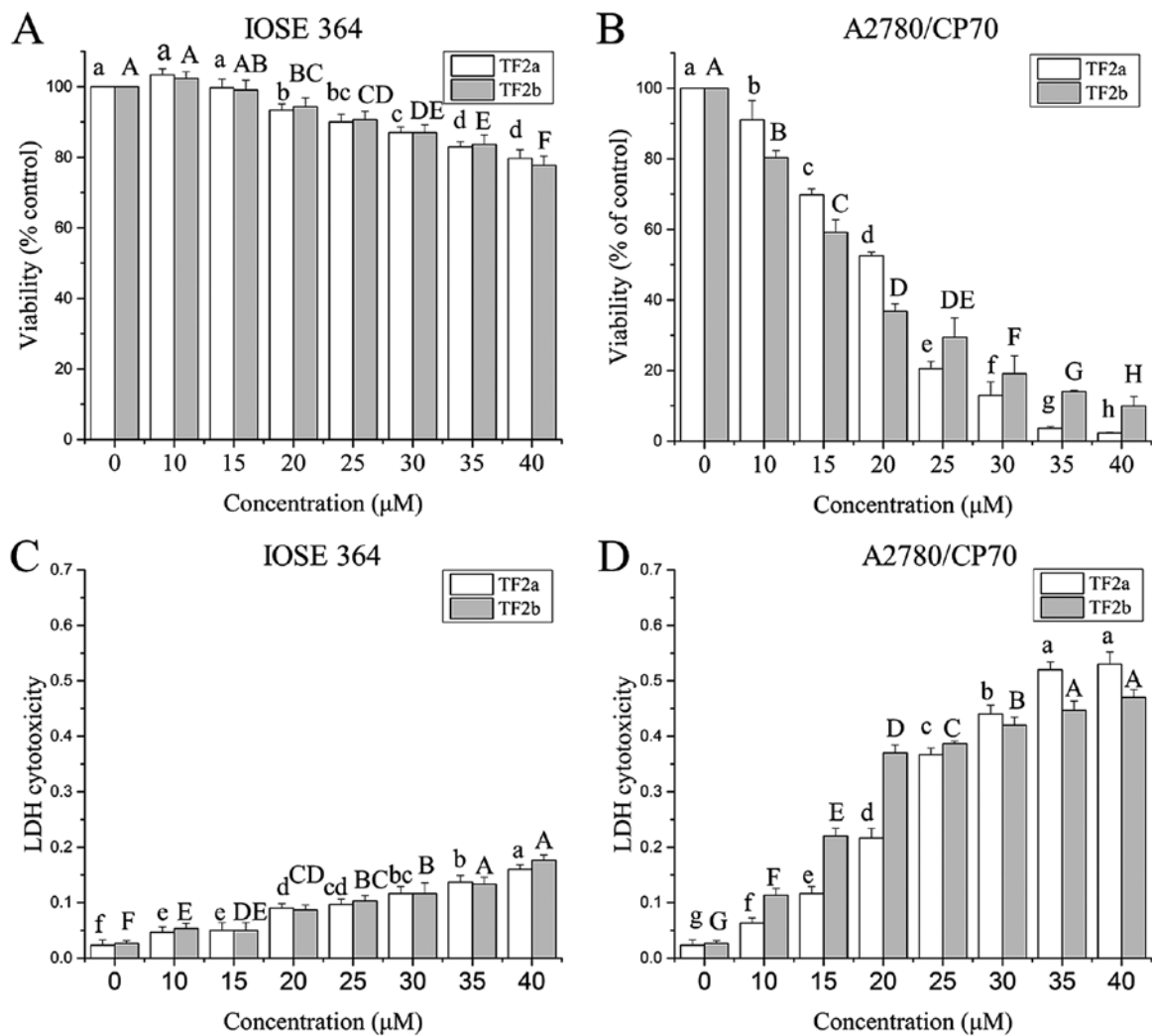
Figure 1. TF2a and TF2b inhibit cell viability and induce cytotoxicity in IOSE-364 cells and A2780/CP70 cells. Effect of TF2a and TF2b on cell viability of IOSE-364 cells (A) and A2780/CP70 cells (B) was determined using the MTS assay after treatment with the designated concentrations (0-40 μM) of TF2a and TF2b for 24 h. LDH cytotoxicity of TF2a and TF2b on IOSE-364 cells (C) and A2780/CP70 cells (D) were determined by LDH assay after treatment with various concentrations of TF2a and TF2b for 24 h. Results are expressed as mean ± SD from three independent experiments. Significant differences among different treatments are marked with different letters (p<0.05).

West Dura Extended Duration Substrate (Life Technologies) and ChemiDoc™ MP System (Bio-Rad, Hercules, CA, USA). Protein bands were analyzed with ImageJ software and normalized with GAPDH.

Silence with small interfering RNA (siRNA). A2780/CP70 cells were seeded in 60-mm dishes at 5x10^5 cells/dish and incubated overnight. Then the cells were transfected with p53 siRNA (Santa Cruz Biotechnology, Inc., Danvers, MA, USA) in Lipofectamine 2000 transfection reagent (Invitrogen) for 24 h according to the manufacturer's protocol. The control cells were transfected with control siRNA (Santa Cruz, Danvers, MA, USA). Then cells were treated with TF2a and TF2b (0, 5, 10 and 20 μM) for 24 h. Cell viability was determined and western blot analysis was carried out.

Statistical analysis. In the present study, all samples were analyzed in triplicate. The data are presented as mean ± standard deviations (SD). Multiple comparisons were analyzed by least significant difference (LSD) test. Statistical differences

between two groups were analyzed with Student's t-test. All statistical analysis was carried out using Statistical Analysis system. p<0.05 and p<0.01 were considered statistically significant and highly significant, respectively.

Results

Effect of TF2a and TF2b on A2780/CP70 cell viability. Ovarian cancer A2780/CP70 cell line and normal ovarian epithelial IOSE-364 cell line were used to investigate the effect of TF2a and TF2b on ovarian cells. The anti-proliferation effect of TF2a and TF2b on A2780/CP70 and IOSE-364 was evaluated using the MTS assay. As shown in Fig. 1A and B, TF2a and TF2b inhibited the proliferation of the cells in a dose-dependent manner. The cell viability ranged from 100 to 2.32% for TF2a treatment, and from 100 to 9.95% for TF2b treatment. The IC$_{50}$ values of TF2a and TF2b against A2780/CP70 cells were 18.1 and 17.2 μM, respectively. In contrast, TF2a and TF2b had relatively moderate cytotoxic effect on IOSE-364 cells. The least viability of IOSE 364 cells was 79.67% for
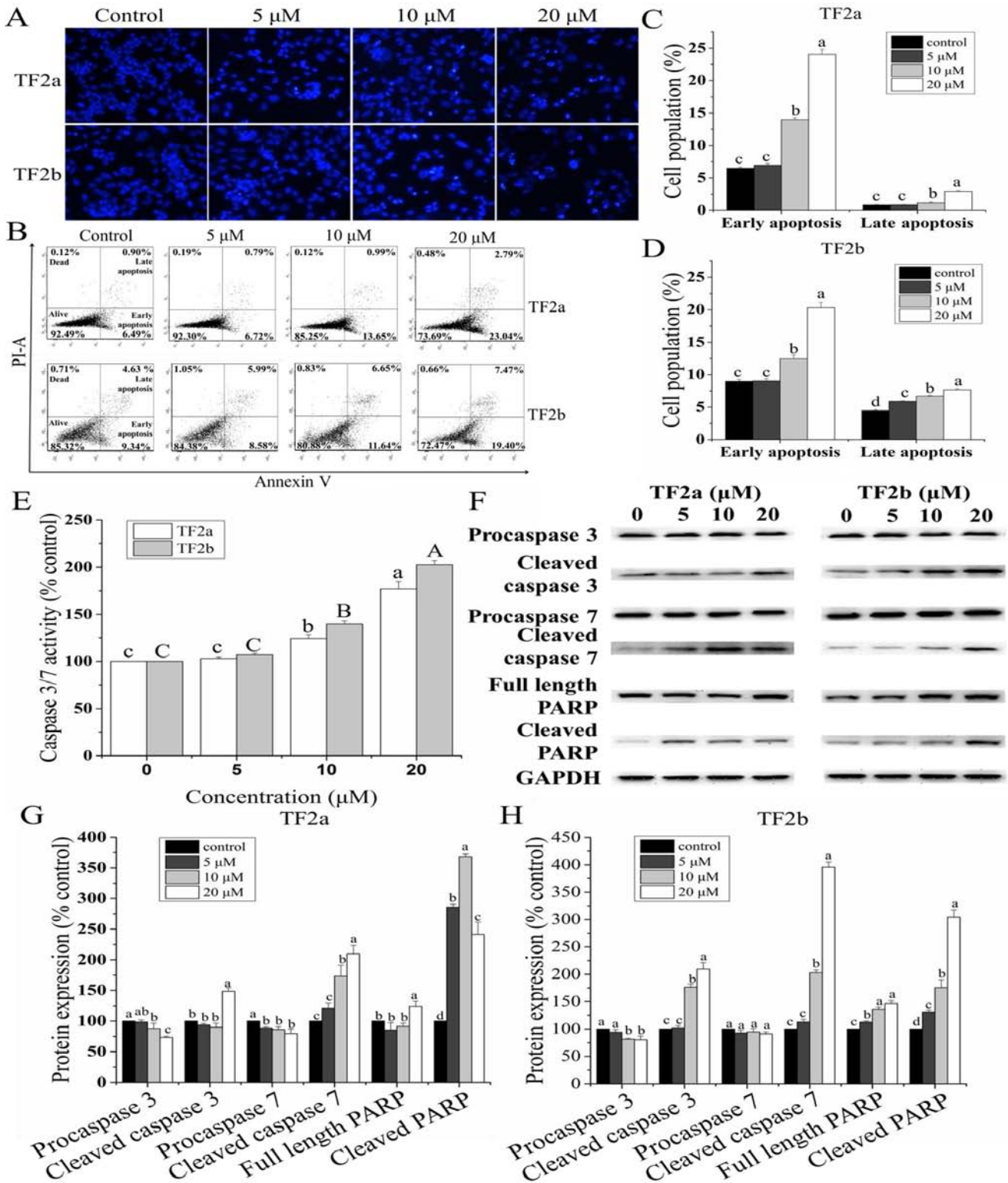
Figure 2. TF2a and TF2b induce apoptosis in A2780/CP70 cells. (A) A2780/CP70 cells stained with Hoechst 33342 were detected by fluorescent microscopy (magnification, x400) after treatment with designated concentrations (0, 5, 10 and 20 μM) of TF2a and TF2b for 24 h. The bright nuclei represent apoptotic cells. Intact nuclei represent viable cells. (B) Flow cytometric analysis of A2780/CP70 cells after treatment with various concentrations of TF2a and TF2b for 24 h. Data of apoptosis induced by TF2a (C) and TF2b (D) were expressed as quantification histograms with error bars. (E) Caspase-3/7 activity was determined after treatment with various concentrations of TF2a and TF2b for 24 h. The caspase-3/7 activity of control cells was expressed as 100%. (F) Protein expression levels of procaspase-3, cleaved caspase-3, procaspase-7, cleaved caspase-7, full length PARP and cleaved PARP were analyzed by western blotting. The changes of the protein expression induced by TF2a (G) and TF2b (H) were expressed as quantification histograms with error bars. Results are expressed as mean ± SD from three independent experiments. Significant differences among different treatments are marked with different letters (p<0.05).

TF2a and 77.67% for TF2b after 40 μM TF2a and TF2b treatment for 24 h.

To further investigate the cytotoxicity effect of TF2a and TF2b against A2780/CP70 and IOSE-364 cells, LDH

cytotoxicity was evaluated. As shown in Fig. 1C and D, TF2a and TF2b induced cytotoxicity of the cells after treatment (0-40 μM) for 24 h in a dose-dependent manner. TF2a and TF2b induced dramatic LDH release in A2780/CP70 cells as the treatment concentration increased. TF2a and TF2b induced 23.0 and 17.4 times more LDH release than that of control in A2780/CP70 cells at the concentration of 40 μM. However, TF2a and TF2b induced slight LDH release in IOSE-364. TF2a and TF2b induced 6.7 and 6.5 times more LDH release than that of control in IOSE364 cells at the concentration of 40 μM. As the viability and cytotoxicity results showed, TF2a and TF2b had higher cytotoxic effect against ovarian cancer A2780/CP70 cells than those against normal ovarian IOSE-364 cells.

TF2a and TF2b induce apoptosis in A2780/CP70 cells. To study whether TF2a and TF2b induced apoptosis resulting in cell viability inhibition and cell cytotoxicity, the changes of nuclear morphology in A2780/CP70 cells treated with TF2a and TF2b (0, 5, 10 and 20 μM) were evaluated using Hoechst 33342 DNA staining. As showed in Fig. 2A, the nuclei in control cells were intact, and appeared less bright. With treatment of TF2a and TF2b, the apoptotic cells were stained much brighter with condensed or fragmented nuclei.

Double staining with Annexin V FITC and PI followed by flow cytometry analysis was also used to investigate the apoptosis induced by TF2a and TF2b. As shown in Fig. 2B-D, the treatment of TF2a and TF2b significantly increased the percentage of early apoptotic cells and late apoptotic cells in a dose-dependent manner (p<0.05). The portion of early apoptotic cells increased from 6.51 to 24.01% for TF2a and from 8.96 to 20.30% for TF2b. The portion of late apoptotic cells increased from 0.85 to 2.93% for TF2a and from 4.48 to 7.66% for TF2b. The total percent of apoptotic cells increased from 7.36 to 26.94% for TF2a and 13.44 to 27.96% for TF2b, respectively.

Caspase-3/7 plays a central role in the execution-phase of cell apoptosis. To confirm that TF2a and TF2b induced apoptosis, we evaluated the caspase-3/7 activities in A2780/CP70 cells. As showed in Fig. 2E, treatment with TF2a and TF2b enhanceed the caspase-3/7 activity by 1.77- and 2.03-fold compared to that in controls, respectively.

Furthermore, the expression of proteins related to apoptosis in A2780/CP70 cells was analyzed by western blot (Fig. 2F-H). As the treatment concentrations of TF2a and TF2b increased, the expression of procaspase-3/7 proteins for TF2a and procaspase-3 proteins for TF2b decreased significantly and the expression of cleaved caspase-3/7, full length PARP and cleaved PARP proteins increased significantly. There was no significant difference in the expression of procaspase-7 proteins for TF2b. Taken together, these results indicated that TF2a and TF2b can induce apoptosis in A2780/CP70 cells.

TF2a and TF2b induce G1 cell cycle arrest in A2780/CP70 cells. To investigate whether the anti-proliferative effect of TF2a and TF2b against A2780/CP70 cells was triggered by cell cycle arrest, we analyzed the distribution of cell cycle phase in cells treated with TF2a and TF2b (0, 5, 10 and 20 μM) and

stained with PI using flow cytometry. As shown in Fig. 3A-C, the cell population at the G1 phase was increased in a dose-dependent manner (p<0.05). The percentage of the cells at G1 phase increased from 41.77 to 71.07% for TF2a and from 42.06 to 75.68% for TF2b. In addition, a significant decrease in the proportion of cells at both S and G2 phase was observed. These results suggested that TF2a and TF2b induced G1 cell cycle arrest in A2780/CP70 cells.

To investigate the underlying mechanism of TF2a and TF2b-induced G1 phase arrest in A2780/CP70 cells, the effect of TF2a and TF2b on G1 phase regulatory proteins was evaluated by western blot analysis. As shown in Fig. 3D-F, TF2a could effectively downregulate CDK2 and CDK4 protein expression (p<0.05), upregulate p21 protein expression (p<0.05), but had no effect on the expression of cyclin D1 and cyclin E1 proteins (p>0.05). TF2b could effectively downregulate CDK2 and cyclin E1 protein expression (p<0.05), upregulate p21 protein expression (p<0.05), but had no effect on the expression of CDK4 and cyclin D1 proteins (p>0.05). These western blot results implied that TF2a and TF2b induced G1 phase arrest in A2780/CP70 cells by downregulating CDK2 and CDK4 protein expression and CDK2 and cyclin E1 protein expression, respectively.

Role of p53 in TF2a and TF2b-induced apoptosis and cell cycle arrest. The p53 signaling pathway plays an important role in cellular response to DNA damage and other genomic aberrations. Activation of p53 leads to either cell cycle arrest and DNA repair or apoptosis (20). To clarify the role of p53 in apoptosis and cell cycle arrest induced by TF2a and TF2b in A2780/CP70 cells after treatment for 24 h, p53 protein expression was determined by western blotting. As shown in Fig. 4A and B, TF2a and TF2b significantly upregulated the protein expression of p53 (p<0.05).

To further analyze the effect of p53 on apoptosis and cell cycle G1 phase arrest induced by TF2a and TF2b, p53 was silenced by siRNA. Pre-incubation of 50 nM p53 siRNA significantly attenuated the inhibitory effect of TF2a and TF2b on A2780/CP70 cells (p<0.05 or 0.01) (Fig. 4C). The expression of p53 protein was markedly inhibited after treatment with 50 nM p53 siRNA (p<0.01) (Fig. 4D-F). The p53 protein depletion weakened the effect of TF2a and TF2b-induced decrease in CDK2 and procaspase-3 protein expression (p<0.05). These western blot results suggested that p53 played an important role in apoptosis and G1 cell cycle arrest induced by TF2a and TF2b in A2780/CP70 cells.

TF2a and TF2b induce DNA damage in A2780/CP70 cells. The p53 protein plays a major role in cellular response to DNA damage. The cell cycle can be held at the G1 regulation point on DNA damage recognition (21). To determine whether TF2a and TF2b induced DNA damage in A2780/CP70 cells after treatment for 24 h, the levels of DNA damage related proteins including histone H2A.X, p-histone H2A.X (Ser139), ATM, p-ATM (Ser1981), Chk1, Chk2, p-Chk1 (Ser345), p-Chk2 (Thr68) and p-p53 (Ser15) were determined.

The phosphorylation of histone H2A.X at Ser139 indicates DNA double-strand breaks. ATM is autophosphorylated on
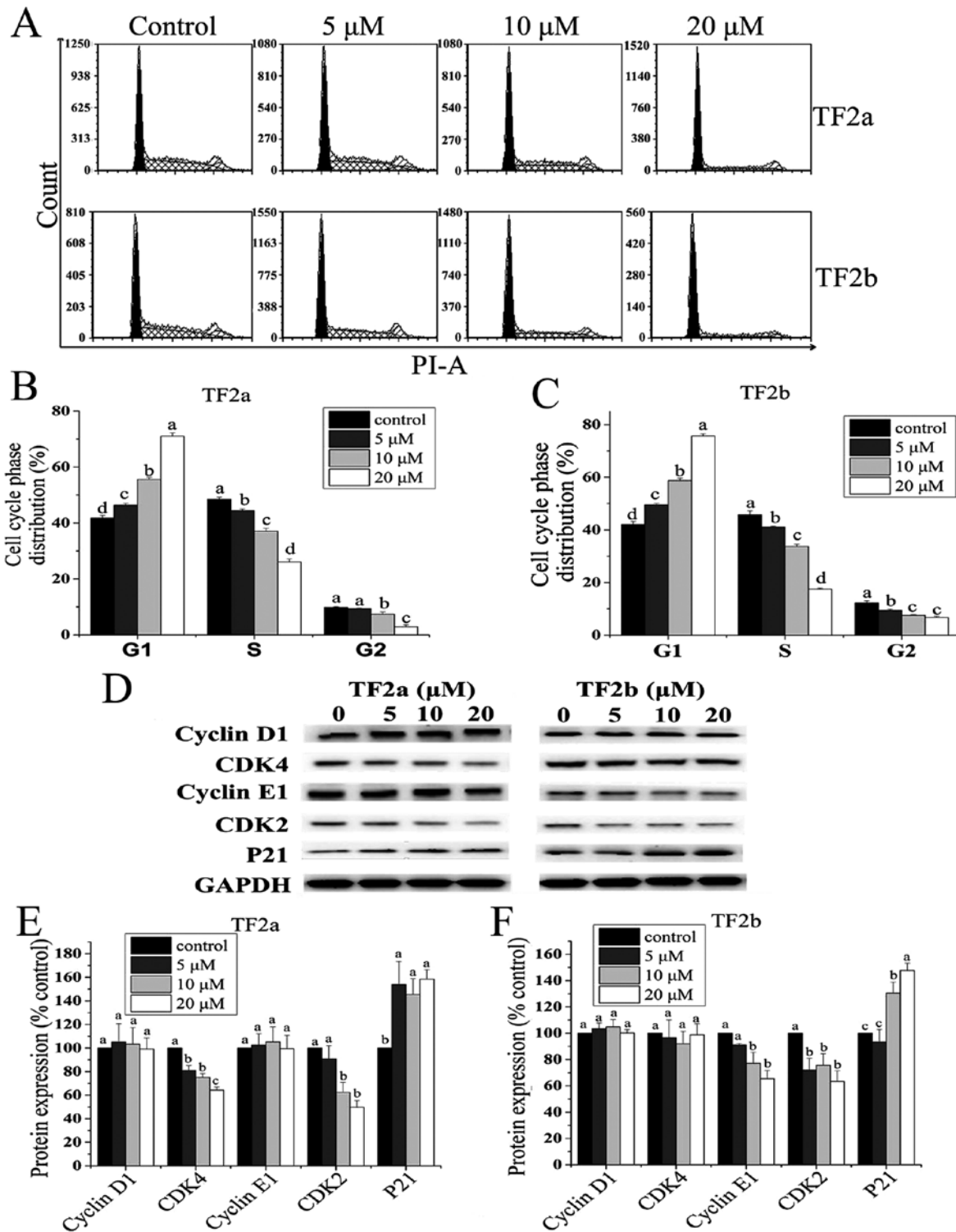
Figure 3. TF2a and TF2b induce cell cycle arrest in A2780/CP70 cells. (A) Cell cycle phase distributions were analyzed in A2780/CP70 cells treated with designated concentrations (0, 5, 10 and 20 μM) of TF2a and TF2b for 24 h. Data of cell cycle phase distribution change induced by TF2a (B) and TF2b (C) were expressed as quantification histograms with error bars. (D) Protein expression levels of cell cycle G1-related proteins, including cyclin D1, CDK4, cyclin E1, CDK2 and p21 were analyzed by western blotting. A2780/CP70 cells were treated with various concentrations of TF2a and TF2b for 24 h. The changes of the protein expression induced by TF2a (E) and TF2b (F) were expressed as quantification histograms with error bars. Results are expressed as mean ± SD from three independent experiments. Significant differences among different treatments are marked with different letters ($p < 0.05$).

Ser1981 in response to DNA damage (22). As shown in Fig. 5, both TF2a and TF2b significantly increased the protein levels of p-histone H2A.X (Ser139), and p-ATM (Ser1981) ($p < 0.05$), but had no effect on the protein level of total histone H2A.X ($p > 0.05$). TF2a significantly increased the

protein level of ATM ($p < 0.05$), but TF2b had no significant effect on the protein expression of ATM ($p > 0.05$). Chk1 and Chk2 can be phosphorylated by p-ATM. Both TF2a and TF2b significantly upregulated the protein levels of p-Chk1 (Ser345) and p-Chk2 (Thr68) ($p < 0.05$), but had
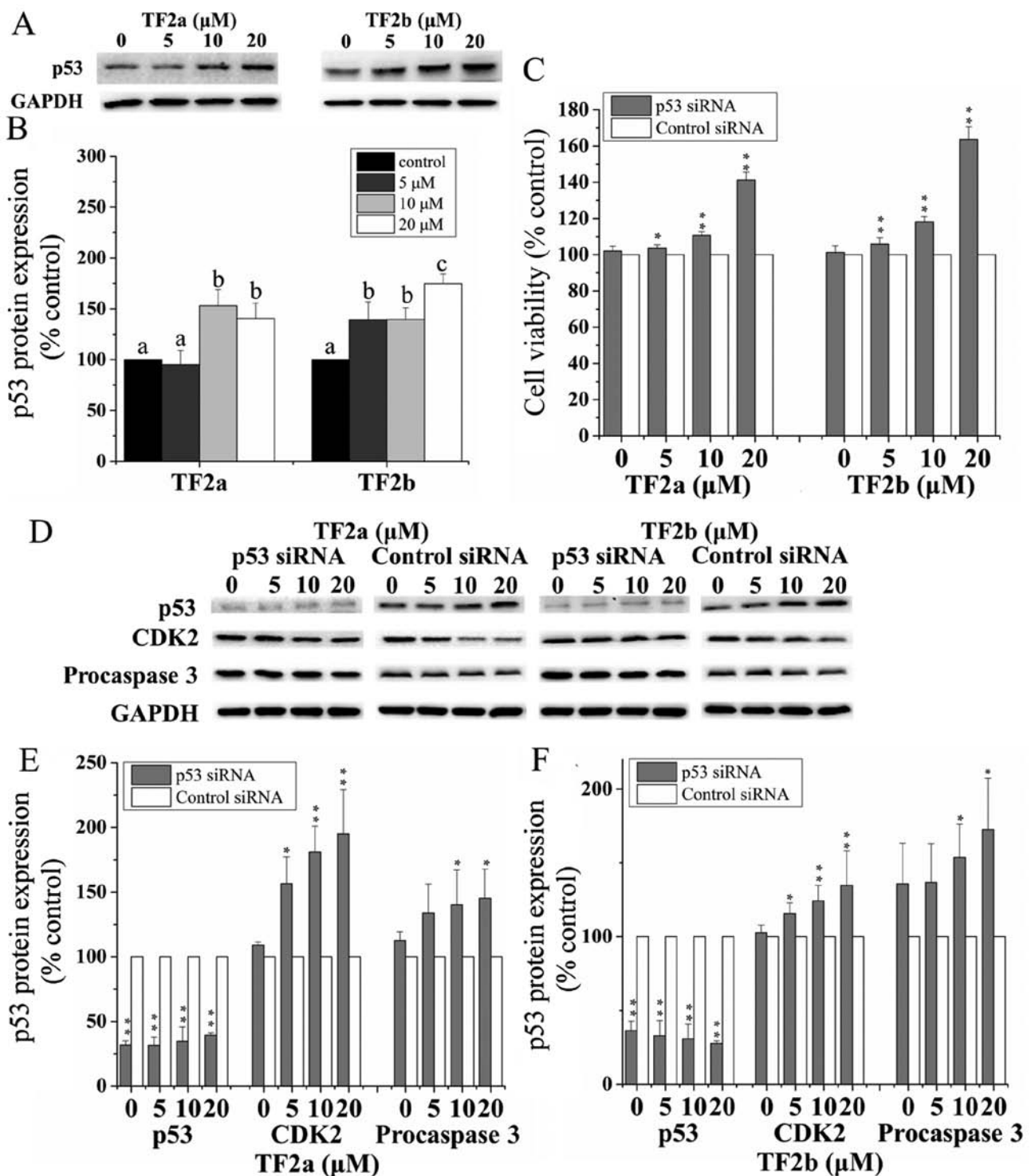
Figure 4. Role of p53 in TF2a and TF2b-induced apoptosis and cell cycle G1 phase arrest in A2780/CP70 cells. (A) The effect of TF2a and TF2b on the p53 protein expression was analyzed by western blotting. (B) The changes of the protein expression induced by TF2a and TF2b were expressed as quantification histograms with error bars. Significant differences among different treatments are marked with different letters ($p<0.05$). (C) The effect of p53 siRNA on the cell viability of A2780/ CP70 cells treated by TF2a and TF2b. Cells were pretreated with 50 nM p53 siRNA for 24 h followed by TF2a and TF2b treatment for 24 h. *$p<0.05$, **$p<0.01$, compared with respective controls. (D) The effect of p53 siRNA (50 nM) on the protein expression of p53, CDK2 and procaspase-3 was analyzed by western blotting. *$p<0.05$, **$p<0.01$, compared with respective controls. Results are expressed as mean ± SD from three independent experiments. After the cells were treated with 50 nM p53 siRNA, the changes of the protein expression induced by TF2a (E) and TF2b (F) were expressed as quantification histograms with error bars. Results are expressed as mean ± SD from three independent experiments. Significant differences among different treatments are marked with different letters ($p<0.05$).

no significant effect on the protein levels of total Chk1/2 ($p>0.05$). The p53 protein can be phosphorylated by ATM, ATR, and DNA-PK at Ser15, promoting both the accumula-

tion and activation of p53 in response to DNA damage (23). Both TF2a and TF2b significantly increased the protein levels of p-p53 (Ser15) ($p<0.05$). It was concluded that TF2a
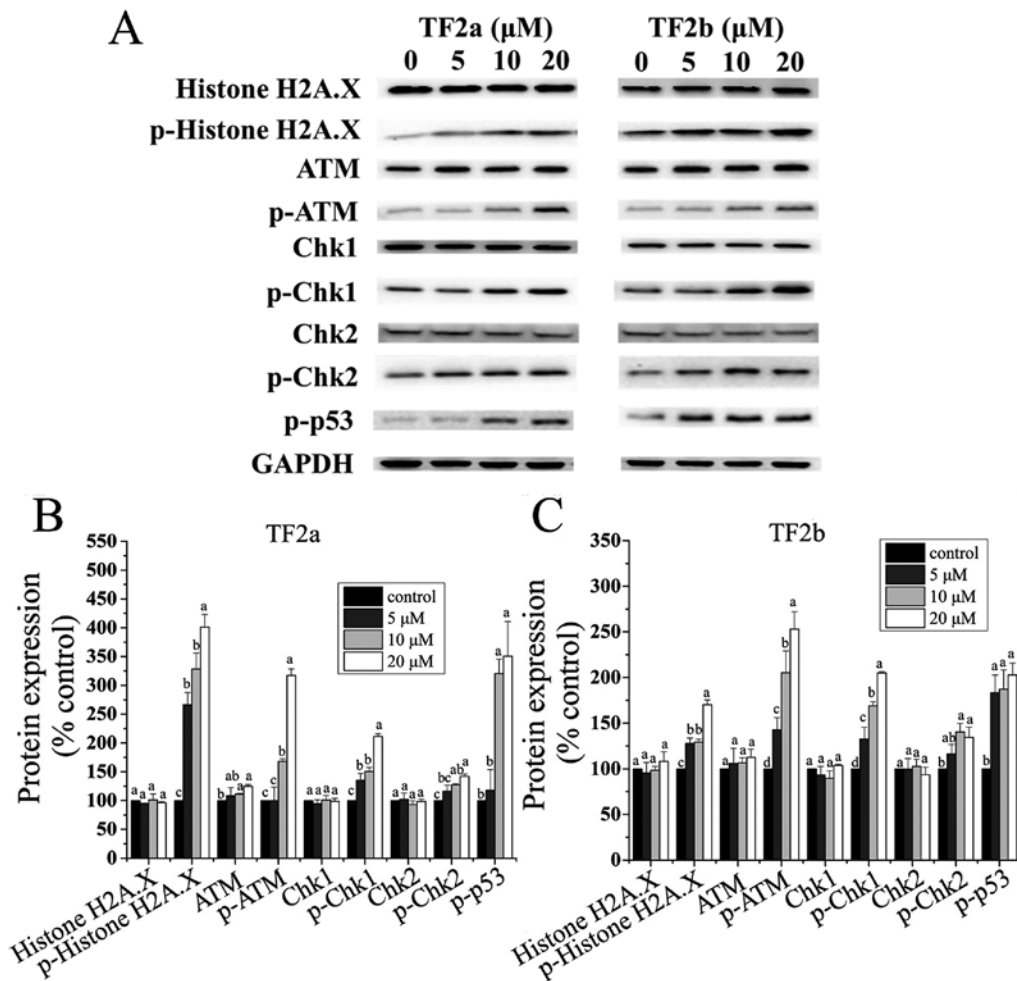
Figure 5. TF2a and TF2b induce DNA damage in A2780/CP70 cells. (A) Protein expression levels of DNA damage-related proteins, including histone H2A.X, p-histone H2A.X (Ser139), ATM, p-ATM (Ser1981), Chk1, Chk2, p-Chk1 (Ser345), p-Chk2 (Thr68) and p-p53 (Ser15) were analyzed by western blotting. A2780/CP70 cells were treated with designated concentrations (0, 5, 10 and 20 μM) of TF2a and TF2b for 24 h. The changes of the protein levels induced by TF2a (B) and TF2b (C) were expressed as quantification histograms with error bars. Results are expressed as mean ± SD from three independent experiments. Significant differences among different treatments are marked with different letters (p<0.05).
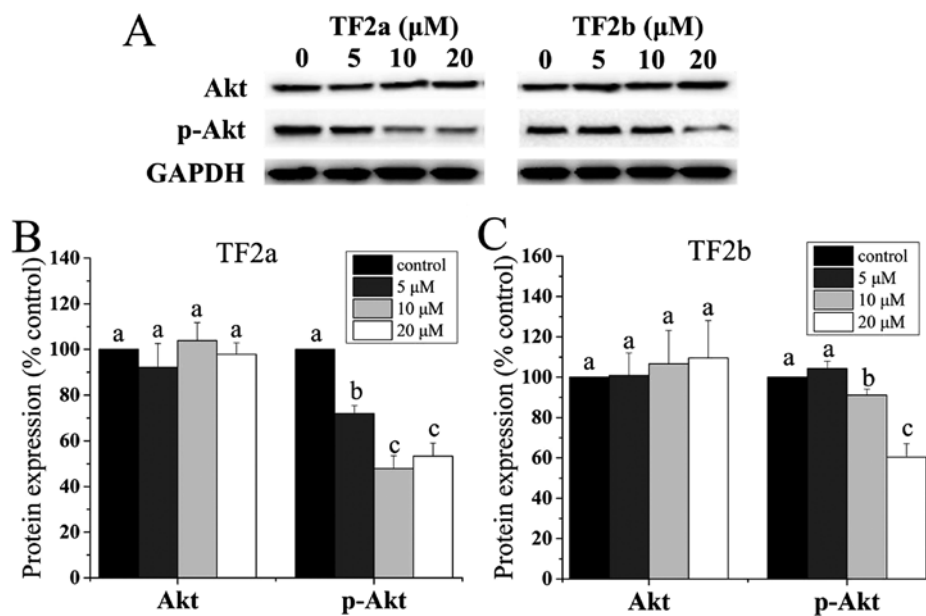

Figure 6. Role of Akts in TF2a and TF2b-induced apoptosis and cell cycle G1 phase arrest in A2780/CP70 cells. (A) Protein expression levels of Akt and p-Akt (Ser473) were analyzed by western blotting. A2780/CP70 cells were treated with designated concentrations (0, 5, 10 and 20 μM) of TF2a and TF2b for 24 h. The changes of the protein expression induced by TF2a (B) and TF2b (C) were expressed as quantification histograms with error bars. Results are expressed as mean ± SD from three independent experiments. Significant differences among different treatments are marked with different letters (p<0.05).
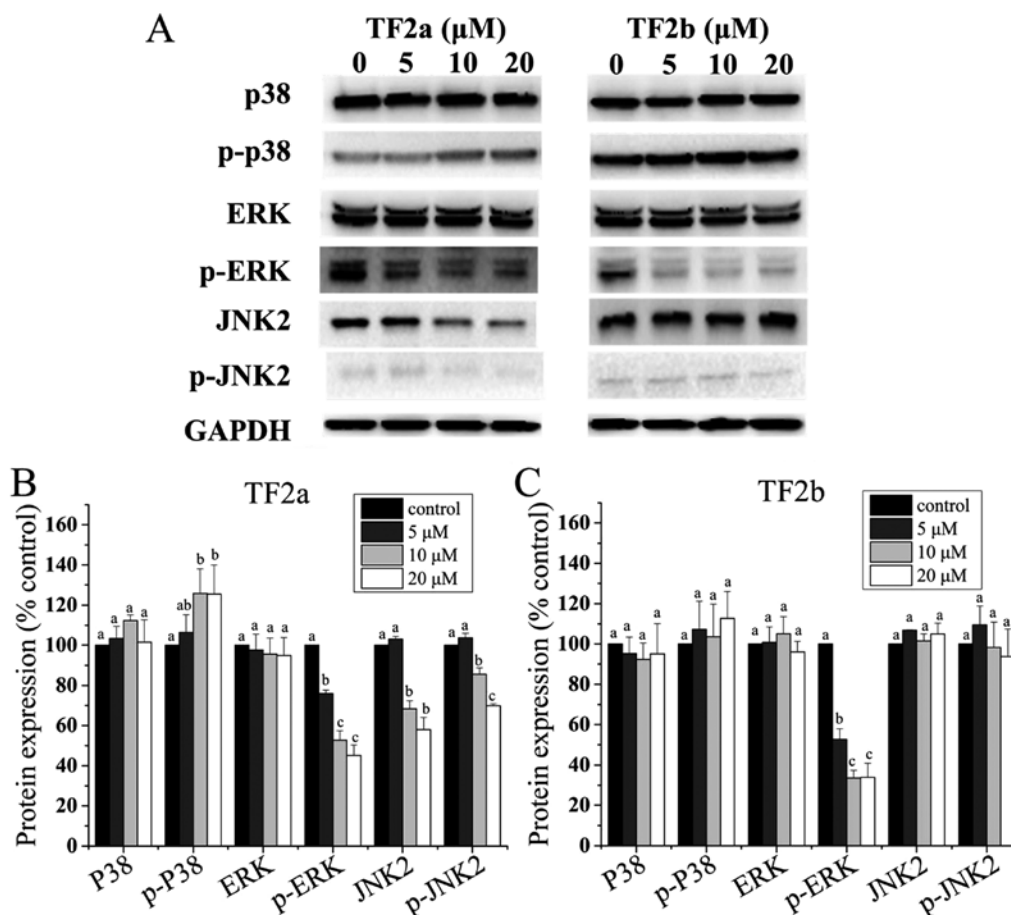
Figure 7. Role of MAPKs in TF2a and TF2b-induced apoptosis and G1 cell cycle arrest in A2780/CP70 cells. (A) Protein expression levels of p38, p-p38, ERK1/2, p-ERK1/2, JNK1/2 and p-JNK1/2 were analyzed by western blotting. A2780/CP70 cells were treated with designated concentrations (0, 5, 10 and 20 μM) of TF2a and TF2b for 24 h. The changes of the protein expression induced by TF2a (B) and TF2b (C) were expressed as quantification histograms with error bars. Results are expressed as mean ± SD from three independent experiments. Significant differences among different treatments are marked with different letters ($p < 0.05$).

and TF2b induced DNA damage by activating ATM-Chk1 and ATM-Chk2 pathways.

Role of Akt in TF2a and TF2b-induced apoptosis and cell cycle arrest. It was demonstrated that the p53 level is negatively controlled by Akt (24). Akt plays a critical role in controlling survival and apoptosis which is activated through phosphorylation by insulin and various growth and survival factors (25,26). In addition to its role in survival, Akt is involved in cell cycle regulation by preventing GSK-3β-mediated degradation of cyclin D1 (27). Therefore, the protein levels of Akt and p-Akt in A2780/CP70 cells were determined. As shown in Fig. 6, TF2a and TF2b significantly reduced the phosphorylation of Akt and had no influence on the level of total Akt protein ($p < 0.05$).

Role of MAPK in TF2a and TF2b-induced apoptosis and cell cycle arrest. It is clear that the p53 protein can functionally interact with the mitogen-activated protein kinase (MAPK) (28). Therefore, to clarify whether MAPKs mediated apoptosis and cell cycle arrest induced by TF2a and TF2b in A2780/CP70 cells, the levels of p38, p-p38, ERK1/2, p-ERK1/2, JNK1/2 and p-JNK1/2 were determined. As shown in Fig. 7, TF2a increased the phosphorylation of p38 ($p < 0.05$),

but had no effect on the protein expression of p38 ($p > 0.05$). TF2b had no effect on the protein expression of p38 and the phosphorylation of p38 ($p > 0.05$). Both TF2a and TF2b suppressed the phosphorylation of ERK1/2 ($p < 0.05$), but had no effect on the protein expression of ERK1/2 ($p > 0.05$). TF2a suppressed the protein expression of JNK2 and the phosphorylation of JNK2 ($p < 0.05$), but TF2b had no effect on the protein expression of JNK2 and the phosphorylation of JNK2 ($p > 0.05$). The protein expression of JNK1 and p-JNK1 was so low in A2780/CP70 cells that they were not detected by western blotting (Fig. 7).

Discussion

Ovarian cancer is the most lethal gynecological malignancy. Cisplatin and its derivatives are first-line chemotherapeutic agents in the treatment of ovarian cancer, and their resistance and adverse side effects are major barriers in successful ovarian cancer treatment (2). Theaflavins showed effective inhibition of ovarian cancer and were less cytotoxic to normal ovarian IOSE-364 cells (18). Hence, the possible mechanisms underlying these modulations of TF2a and TF2b against ovarian cancer cells stimulated our interest. In the present study, we found that the IC$_{50}$ values of TF2a and TF2b against

A2780/CP70 cells were 18.1 and 17.2 μM, which were much lower than those against IOSE-364 cells (Fig. 1). In LDH assay, significant LDH leakage was observed in ovarian cancer cell lines while slight LDH release was induced in IOSE-364 cells (Fig. 1). The MTS and LDH assays suggested the effect of TF2a and TF2b against ovarian cancer cells and normal ovarian cells was different. Conventional chemotherapy although cytotoxic, does not discriminate cancer and normal cells. An ideal anti-cancer drug is expected to be selective and cytotoxic to cancer cells but less cytotoxic to normal cells (29). TF2a and TF2b were demonstrated to be selective and cytotoxic to ovarian carcinoma A2780/CP70 cell line and less cytotoxic to normal ovarian surface epithelial IOSE-364 cell line. The selective cell growth inhibitory effect maybe partly attributed to the apoptosis and G1 cell cycle arrest induced by TF2a and TF2b.

One mechanism by which cancer cells develop resistance to chemotherapeutic agents and radiation is correlated with their resistance to apoptosis. Thus, apoptosis induced by TF2a and TF2b in ovarian cancer cells was evaluated using several methods. Morphological hallmarks of apoptosis in the nucleus are chromatin condensation and nuclear fragmentation (30). The changes were clearly observed in ovarian cancer cells after treatment with TF2a and TF2b by Hoechst 33342 staining. TF2a and TF2b rendered condensed and fragmented nuclei brighter in a dose-dependent manner (Fig. 2A). Loss of plasma membrane asymmetry is another morphological hallmark of apoptosis (31) which was observed in ovarian cancer cells after treatment with TF2a and TF2b by Annexin V/PI staining. TF2a and TF2b increased the percent of both early and late apoptotic cells in a dose-dependent manner (Fig. 2B-D). Caspases are central to the mechanism of apoptosis as they are both the initiators and executioners. Caspases involved in apoptosis have been classified by their mechanism of action and are either initiator caspases (caspase-8 and -9) or executioner caspases (caspase-3 and -7) (32). Activation of caspase-3 and -7 requires proteolytic processing of the inactive zymogen into activated fragments. Caspase-3 and -7 activities and protein levels of caspase-3 and -7 in ovarian cancer cells after treatment with TF2a and TF2b were determined. TF2a and TF2b increased the caspase-3 and -7 activities (Fig. 2E) and protein levels of cleaved caspase-3 and -7 (Fig. 2F-H). As cleavage of procaspase-3 and -7 increased, the protein levels of procaspase-3 and -7 decreased. PARP is involved in a number of cellular processes such as DNA repair, genomic stability, and programmed cell death. Cleaved PARP serves as a marker of cells undergoing apoptosis (33-35). The protein level of cleaved PARP increased after treatment with TF2a and TF2b in a dose-dependent manner. Taken together, all these results indicated that TF2a and TF2b inhibited ovarian cancer cells by inducing apoptosis.

Cell cycle regulation plays an important role in tumorigenesis and tumor progression (36). Cell cycle arrest is important for determining toxicities and responses to current cancer therapies (37). Cell cycle arrest may be attributed partly to the inhibitory effect of TF2a and TF2b on ovarian cancer cells. Flow cytometric analysis demonstrated that TF2a and TF2b induced cell cycle G1 phase arrest in A2780/CP70 cells after TF2a and TF2b treatment (Fig. 3A-C). Previous studies have reported that theaflavins induced cell cycle G1 phase arrest in a variety of cancer cells such as rat hepatoma AH109A

cells (38) and murine B16 melanoma cells (38) and cell cycle G2 phase arrest in a variety of cancer cells including human prostate carcinoma PC-3 cells (39) and human ovarian cancer A2780/CP70 cells (16). To further investigate the underlying mechanism of TF2a and TF2b-induced cell cycle G1 arrest, the protein levels of G1-related regulatory proteins were determined. The G1 checkpoint arrests the cell cycle by inhibiting this G1-S transition machinery. It usually arrests the cell cycle G1 phase by inhibiting cyclin E-CDK2 and cyclin D-CDK4 complex (40). The p21 protein is a potent cyclin-dependent kinase inhibitor, which is necessary for the p53-mediated G1 arrest (41) and functions as a regulator of cell cycle progression at G2 phase (42). In the present study, TF2a and TF2b induced G1 arrest in A2780/CP70 cells by downregulating CDK2 and CDK4 protein expression and CDK2 and cyclin E1 protein expression, respectively (Fig. 3D-F). The p21 protein level was upregulated by TF2a and TF2b. TF2a could not influence the protein expression of cyclin D1 and cyclin E1 and TF2b could not influence the protein expression of CDK4 and cyclin D1. The results indicated CDK2 and CDK4 for TF2a and CDK2 and cyclin E for played an important role in cell cycle G1 arrest of A2780/CP70 cells.

The p53 tumor suppressor protein plays a major role in cellular response to DNA damage and other genomic aberrations. Since over 50% of human cancers carry loss of function mutations in p53 gene, p53 is considered to be one of the classical type tumor suppressors. Activation of wild-type p53 can lead to either cell cycle arrest and DNA repair or apoptosis that help to prevent tumor development (43,44). It is known that the p53 gene sequence in A2780/CP70 cell line is wild-type (45). Our data showed TF2a and TF2b significantly increased the protein expression of p53 (Fig. 4A and B). Furthermore, silencing by the p53 siRNA significantly attenuated the inhibitory effect of TF2a and TF2b on A2780/CP70 cells and abrogated TF2a and TF2b-induced decrease in CDK2 and procaspase-3 protein expression. These results suggested that p53 played an important role in apoptosis and G1 cell cycle arrest induced by TF2a and TF2b in A2780/CP70 cells. It has been reported that p53 could mediate apoptosis induced by theaflavins in human breast and prostate cancer cells which was consistent with results in the present study (46,47).

Activation of p53 can occur in response to DNA damage. Several forms of DNA damage have been shown to activate p53, including those generated by ionising radiation, radio-mimetic drugs, ultraviolet light and chemicals (48). ATM is a sensor of DNA damage caused by ionizing radiation, UV-light, or radio-mimetic agents, of which activation by autophosphorylation at Ser1981 occurs in response to exposed DNA double-stranded breaks (49). Chk1/2 acts downstream of ATM and plays an important role in DNA damage checkpoint control. Chk1 at Ser345 (50) and Chk2 at Thr68 (51,52) are phosphorylated by ATM in response to DNA damage, histone H2A.X is required for checkpoint-mediated cell cycle arrest and DNA repair following DNA double-stranded breaks (53). DNA damage results in rapid phosphorylation of histone H2A.X at Ser139 by ATM (22,54). ATM can phosphorylate p53 at Ser15, which impaired the ability of MDM2 to bind p53 and promoted both the accumulation and activation of p53 in response to DNA damage (23,55). In the present study, TF2a and TF2b upregulated the phosphorylation of ATM at Ser1981, histone H2A.X at

Ser139, Chk1 at Ser345 and Chk2 at Thr68 (Fig. 5) which indicated DNA double-stranded break occurred in A2780/CP70 cells. Total p53 protein and phosphorylation of p53 at Ser15 were markedly increased in a dose-dependent manner, which also suggested DNA damage occurred in A2780/CP70 cells. Previous studies reported that activation of ATM/Chk/p53 pathway could induce apoptosis in human pancreatic cancer BxPC-3 cells (56) and cell cycle G1 arrest in A549 lung cancer cells (57). Our results suggested that this pathway was involved in TF2a and TF2b-induced apoptosis and cell cycle G1 phase arrest in A2780/CP70 cells.

Akt is a serine/threonine kinase that plays an important role in the development and progression of cancers (58). This protein kinase is activated by insulin and various growth and survival factors (59). The AKT pathway is one of the most frequently hyperactivated signaling pathways in human cancers. Inhibition of Akt pathway may be a helpful and potential cancer therapy (60). Akt could mediate negative control of p53 levels through enhancing MDM2-mediated targeting of p53 for degradation (61). It was reported that inhibition of p-Akt sensitized cancer cells to cisplatin in a p53-dependent manner (62). Our data showed that TF2a and TF2b significantly inhibited the phosphorylation of Akt (Fig. 6), indicating that TF2a and TF2b might increase the protein expression of p53 by inactivating Akt in A2780/CP70 cells. It has been reported that TF3 targeted Akt pathways to induce apoptosis in human ovarian cancer A2780/CP70 cells (16). Our results suggest Akt pathway was involved in TF2a and TF2b-induced apoptosis and G1 phase arrest in A2780/CP70 cells.

The p53 protein can functionally interact with the MAPK pathways (28). Upon exposure to stressful stimuli, MAPKs phosphorylate and activate p53, leading to p53-mediated cellular responses. MAPKs function in protein kinase cascades that play a critical role in the regulation of cell growth and differentiation, and control of cellular responses to cytokines and stress. In this study, TF2a increased the phosphorylation of p38, but TF2b had no effect on the phosphorylation of p38 (Fig. 7). Both TF2a and TF2b suppressed the phosphorylation of Erk1/2. TF2a suppressed the phosphorylation of JNK2 ($p<0.05$), but TF2b had no effect on the phosphorylation of JNK2. It was reported that dysregulation of p38 MAPK levels in patients were associated with advanced stages and short survival in cancer patients (63). Inhibition of p38 MAPK was correlated with the resistance to anoikis, which allowed circulating cancer cells to survive (64). The p38 activation in breast cancer cells inhibited tumor metastasis (65). The Erk pathway is activated in >30% of human cancers. Inhibition of Erk pathway is an attractive strategy for cancer therapy. It was reported that small-molecule ERK pathway inhibitors such as BAY 43-9006, PD184352, PD0325901 and ARRY-142886 have reached the clinical trial stage (66). A previous study reported theaflavins inhibited tumor promoter-induced activator protein 1 activation and cell transformation through the inhibition of a JNK-dependent pathway (67). It was also found that JNK inhibition led to antitumor activity in ovarian cancers (68) and was associated with longer progression-free survival of patients with ovarian cancer (69). Our results suggest TF2a could induce apoptosis and G1 phase arrest through p38, Erk and JNK pathways and TF2b could induce apoptosis and G1 phase arrest through ERK pathway.

Adverse side effects and acquired resistance to conventional chemotherapy based on platinum have become major barriers in successful ovarian cancer treatment, and drive the development of other selective anticancer drugs. Our study demonstrated that TF2a and TF2b exhibited a potent growth inhibitory effect in cisplatin-resistant ovarian cancer A2780/CP70 cells and were less cytotoxic to the normal ovarian cell line IOSE-364. TF2a and TF2b induced apoptosis and cell cycle G1 phase arrest in ovarian cancer A2780/CP70 cells. Downregulation of CDK2 and CDK4 for TF2a and CDK2 and cyclin E1 for TF2b led to the accumulation of cells in G1 phase. TF2a and TF2b induced apoptosis and G1 through p53-dependent pathways. TF2a and TF2b induced DNA damage through ATM/Chk/p53 pathway. TF2a and TF2b induced inhibition of Akt pathway. As for MAPK pathways, TF2a activated p38 pathway and suppressed Erk and JNK pathways and TF2b only suppressed Erk pathway without activating the p38 pathway. Our findings help elucidate the mechanisms by which TF2a and TF2b may contribute to the prevention and treatment of platinum-resistant ovarian cancer. TF2a and TF2b would be potential compounds for treating platinum-resistant ovarian cancer.

References

1. Siegel RL, Miller KD and Jemal A: Cancer statistics, 2016. CA Cancer J Clin 66: 7-30, 2016.
2. Ali AY, Farrand L, Kim JY, Byun S, Suh JY, Lee HJ and Tsang BK: Molecular determinants of ovarian cancer chemoresistance: New insights into an old conundrum. Ann NY Acad Sci 1271: 58-67, 2012.
3. Limtrakul P, Pitchakarn P and Suzuki S: Kuguacin J, a Triterpenoid from *Momordica charantia* Linn: A Comprehensive Review of Anticarcinogenic Properties. INTECH Open Access Publisher. DOI: 10.5772/55532, 2013.
4. Al Rawahi T, Lopes AD, Bristow RE, Bryant A, Elattar A, Chattopadhyay S and Galaal K: Surgical cytoreduction for recurrent epithelial ovarian cancer. Cochrane Database Syst Rev Feb 28;(2): CD008765. DOI: 10.1002/14651858.CD008765.pub3, 2013.
5. Wang V, Li C, Lin M, Welch W, Bell D, Wong YF, Berkowitz R, Mok SC and Bandera CA: Ovarian cancer is a heterogeneous disease. Cancer Genet Cytogenet 161: 170-173, 2005.
6. Cragg DJ, Kingston GM and Newman DG (eds): Anticancer Agents from Natural Products. CRC Press, 2011.

7. Butler MS, Robertson AA and Cooper MA: Natural product and natural product derived drugs in clinical trials. Nat Prod Rep 31: 1612-1661, 2014.
8. Newman DJ and Cragg GM: Natural products as sources of new drugs from 1981 to 2014. J Nat Prod 79: 629-661, 2016.
9. Goldbohm RA, Hertog MG, Brants HA, van Poppel G and van den Brandt PA: Consumption of black tea and cancer risk: A prospective cohort study. J Natl Cancer Inst 88: 93-100, 1996.
10. Cassidy A, Huang T, Rice MS, Rimm EB and Tworoger SS: Intake of dietary flavonoids and risk of epithelial ovarian cancer. Am J Clin Nutr 100: 1344-1351, 2014..
11. Finger A: In vitro studies on the effect of polyphenol oxidase and peroxidase on the formation of polyphenolic black tea constituents. J Sci Food Agric 66: 293-305, 1994.
12. Yang GY, Liu Z, Seril DN, Liao J, Ding W, Kim S, Bondoc F and Yang CS: Black tea constituents, theaflavins, inhibit 4-(methylnitrosamino)-1- (3-pyridyl)-1-butanone (NNK)-induced lung tumorigenesis in A/J mice. Carcinogenesis 18: 2361-2365, 1997.
13. Lu J, Ho C-T, Ghai G and Chen KY: Differential effects of theaflavin monogallates on cell growth, apoptosis, and Cox-2 gene expression in cancerous versus normal cells. Cancer Res 60: 6465-6471, 2000.
14. Hibasami H, Komiya T, Achiwa Y, Ohnishi K, Kojima T, Nakanishi K, Sugimoto Y, Hasegawa M, Akatsuka R and Hara Y: Black tea theaflavins induce programmed cell death in cultured human stomach cancer cells. Int J Mol Med 1: 725-727, 1998.
15. Lahiry L, Saha B, Chakraborty J, Adhikary A, Mohanty S, Hossain DM, Banerjee S, Das K, Sa G and Das T: Theaflavins target Fas/caspase-8 and Akt/pBad pathways to induce apoptosis in p53-mutated human breast cancer cells. Carcinogenesis 31: 259-268, 2010.
16. Tu Y, Kim E, Gao Y, Rankin GO, Li B and Chen YC: Theaflavin-3, 3'-digallate induces apoptosis and G2 cell cycle arrest through the Akt/MDM2/p53 pathway in cisplatin-resistant ovarian cancer A2780/CP70 cells. Int J Oncol 48: 2657-2665, 2016.
17. Gao Y, Rankin GO, Tu Y and Chen YC: Theaflavin-3, 3'-digallate decreases human ovarian carcinoma OVCAR-3 cell-induced angiogenesis via Akt and Notch-1 pathways, not via MAPK pathways. Int J Oncol 48: 281-292, 2016.
18. Gao Y, Rankin GO, Tu Y and Chen YC: Inhibitory Effects of the Four Main Theaflavin Derivatives Found in Black Tea on Ovarian Cancer Cells. Anticancer Res 36: 643-651, 2016.
19. Xu Y, Jin Y, Wu Y and Tu Y: Isolation and purification of four individual theaflavins using semi-preparative high performance liquid chromatography. J Liq Chromatogr Relat Technol 33: 1791-1801, 2010.
20. Levine AJ: p53, the cellular gatekeeper for growth and division. Cell 88: 323-331, 1997.
21. Lakin ND and Jackson SP: Regulation of p53 in response to DNA damage. Oncogene 18: 7644-7655, 1999.
22. Burma S, Chen BP, Murphy M, Kurimasa A and Chen DJ: ATM phosphorylates histone H2AX in response to DNA double-strand breaks. J Biol Chem 276: 42462-42467, 2001.
23. Tibbetts RS, Brumbaugh KM, Williams JM, Sarkaria JN, Cliby WA, Shieh SY, Taya Y, Prives C and Abraham RT: A role for ATR in the DNA damage-induced phosphorylation of p53. Genes Dev 13: 152-157, 1999.
24. Gottlieb TM, Leal JFM, Seger R, Taya Y and Oren M: Cross-talk between Akt, p53 and Mdm2: Possible implications for the regulation of apoptosis. Oncogene 21: 1299-1303, 2002.
25. Franke TF, Kaplan DR and Cantley LC: PI3K: Downstream AKTion blocks apoptosis. Cell 88: 435-437, 1997.
26. Franke TF, Yang S-I, Chan TO, Datta K, Kazlauskas A, Morrison DK, Kaplan DR and Tsichlis PN: The protein kinase encoded by the Akt proto-oncogene is a target of the PDGF-activated phosphatidylinositol 3-kinase. Cell 81: 727-736, 1995.
27. Diehl JA, Cheng M, Roussel MF and Sherr CJ: Glycogen synthase kinase-3β regulates cyclin D1 proteolysis and subcellular localization. Genes Dev 12: 3499-3511, 1998.
28. Wu GS: The functional interactions between the p53 and MAPK signaling pathways. Cancer Biol Ther 3: 156-161, 2004.
29. Blagosklonny MV: Overcoming limitations of natural anticancer drugs by combining with artificial agents. Trends Pharmacol Sci 26: 77-81, 2005.
30. Wong RS: Apoptosis in cancer: From pathogenesis to treatment. J Exp Clin Cancer Res 30: 87, 2011.
31. Hassan M, Watari H, AbuAlmaaty A, Ohba Y and Sakuragi N: Apoptosis and molecular targeting therapy in cancer. BioMed Res Int 2014: 150845, 2014.
32. McIlwain DR, Berger T and Mak TW: Caspase functions in cell death and disease. Cold Spring Harb Perspect Biol 7: 7, 2015.
33. Knaapen M, De Bie M, Muhring J and Kockx M: Cleaved PARP as a marker for apoptosis in tissue sections. Promega Notes 72: 7, 1999.
34. Los M, Mozoluk M, Ferrari D, Stepczynska A, Stroh C, Renz A, Herceg Z, Wang ZQ and Schulze-Osthoff K: Activation and caspase-mediated inhibition of PARP: A molecular switch between fibroblast necrosis and apoptosis in death receptor signaling. Mol Biol Cell 13: 978-988, 2002.
35. Morales J, Li L, Fattah FJ, Dong Y, Bey EA, Patel M, Gao J and Boothman DA: Review of poly (ADP-ribose) polymerase (PARP) mechanisms of action and rationale for targeting in cancer and other diseases. Crit Rev Eukaryot Gene Expr 24: 15-28, 2014.
36. Chow A: Cell cycle control by oncogenes and tumor suppressors: Driving the transformation of normal cells into cancerous cells. Nature Education 3: 7, 2010.
37. Sherr CJ and Bartek J: Cell cycle-targeted cancer therapies. Annu Rev Cancer Biol 1: 41-57, 2017.
38. Zhang G, Miura Y and Yagasaki K: Induction of apoptosis and cell cycle arrest in cancer cells by in vivo metabolites of teas. Nutr Cancer 38: 265-273, 2000.
39. Prasad S, Kaur J, Roy P, Kalra N and Shukla Y: Theaflavins induce G2/M arrest by modulating expression of p21$^{waf1/cip1}$, cdc25C and cyclin B in human prostate carcinoma PC-3 cells. Life Sci 81: 1323-1331, 2007.
40. Kawabe T: G2 checkpoint abrogators as anticancer drugs. Mol Cancer Ther 3: 513-519, 2004.
41. Waldman T, Kinzler KW and Vogelstein B: p21 is necessary for the p53-mediated G1 arrest in human cancer cells. Cancer Res 55: 5187-5190, 1995.
42. Yu W, Park S-K, Jia L, Tiwary R, Scott WW, Li J, Wang P, Simmons-Menchaca M, Sanders BG and Kline K: RRR-γ-tocopherol induces human breast cancer cells to undergo apoptosis via death receptor 5 (DR5)-mediated apoptotic signaling. Cancer Lett 259: 165-176, 2008.
43. Ozaki T and Nakagawara A: Role of p53 in cell death and human cancers. Cancers (Basel) 3: 994-1013, 2011.
44. Khoo KH, Verma CS and Lane DP: Drugging the p53 pathway: Understanding the route to clinical efficacy. Nat Rev Drug Discov 13: 217-236, 2014.
45. Brown R, Clugston C, Burns P, Edlin A, Vasey P, Vojtěsek B and Kaye SB: Increased accumulation of p53 protein in cisplatin-resistant ovarian cell lines. Int J Cancer 55: 678-684, 1993.
46. Lahiry L, Saha B, Chakraborty J, Bhattacharyya S, Chattopadhyay S, Banerjee S, Choudhuri T, Mandal D, Bhattacharyya A, Sa G, *et al*: Contribution of p53-mediated Bax transactivation in theaflavin-induced mammary epithelial carcinoma cell apoptosis. Apoptosis 13: 771-781, 2008.
47. Kalra N, Seth K, Prasad S, Singh M, Pant AB and Shukla Y: Theaflavins induced apoptosis of LNCaP cells is mediated through induction of p53, down-regulation of NF-kappa B and mitogen-activated protein kinases pathways. Life Sci 80: 2137-2146, 2007.
48. Meek DW: The p53 response to DNA damage. DNA Repair (Amst) 3: 1049-1056, 2004.
49. Lee JH and Paull TT: Activation and regulation of ATM kinase activity in response to DNA double-strand breaks. Oncogene 26: 7741-7748, 2007.
50. Zhao H and Piwnica-Worms H: ATR-mediated checkpoint pathways regulate phosphorylation and activation of human Chk1. Mol Cell Biol 21: 4129-4139, 2001.
51. Matsuoka S, Rotman G, Ogawa A, Shiloh Y, Tamai K and Elledge SJ: Ataxia telangiectasia-mutated phosphorylates Chk2 in vivo and in vitro. Proc Natl Acad Sci USA 97: 10389-10394, 2000.
52. Melchionna R, Chen X-B, Blasina A and McGowan CH: Threonine 68 is required for radiation-induced phosphorylation and activation of Cds1. Nat Cell Biol 2: 762-765, 2000.
53. Yuan J, Adamski R and Chen J: Focus on histone variant H2AX: To be or not to be. FEBS Lett 584: 3717-3724, 2010.
54. Rogakou EP, Pilch DR, Orr AH, Ivanova VS and Bonner WM: DNA double-stranded breaks induce histone H2AX phosphorylation on serine 139. J Biol Chem 273: 5858-5868, 1998.
55. Shieh S-Y, Ikeda M, Taya Y and Prives C: DNA damage-induced phosphorylation of p53 alleviates inhibition by MDM2. Cell 91: 325-334, 1997.
56. Sahu RP, Batra S and Srivastava SK: Activation of ATM/Chk1 by curcumin causes cell cycle arrest and apoptosis in human pancreatic cancer cells. Br J Cancer 100: 1425-1433, 2009.

57. Lee H, Kim Y, Jeong JH, Ryu J-H and Kim W-Y: ATM/CHK/p53 pathway dependent chemopreventive and therapeutic activity on lung cancer by pterostilbene. PLoS One 11: e0162335, 2016.
58. Altomare DA and Testa JR: Perturbations of the AKT signaling pathway in human cancer. Oncogene 24: 7455-7464, 2005.
59. Crowell JA, Steele VE and Fay JR: Targeting the AKT protein kinase for cancer chemoprevention. Mol Cancer Ther 6: 2139-2148, 2007.
60. Mabuchi S, Kuroda H, Takahashi R and Sasano T: The PI3K/AKT/mTOR pathway as a therapeutic target in ovarian cancer. Gynecol Oncol 137: 173-179, 2015.
61. Abraham AG and O'Neill E: PI3K/Akt-mediated regulation of p53 in cancer. Biochem Soc Trans 42: 798-803, 2014.
62. Kim CW, Lu JN, Go S-I, Jung JH, Yi SM, Jeong JH, Hah YS, Han MS, Park JW, Lee WS, et al: p53 restoration can overcome cisplatin resistance through inhibition of Akt as well as induction of Bax. Int J Oncol 43: 1495-1502, 2013.
63. Koul HK, Pal M and Koul S: Role of p38 MAP kinase signal transduction in solid tumors. Genes Cancer 4: 342-359, 2013.
64. Cheng T-L, Symons M and Jou T-S: Regulation of anoikis by Cdc42 and Rac1. Exp Cell Res 295: 497-511, 2004.
65. Hong B, Li H, Zhang M, Xu J, Lu Y, Zheng Y, Qian J, Chang JT, Yang J and Yi Q: p38 MAPK inhibits breast cancer metastasis through regulation of stromal expansion. Int J Cancer 136: 34-43, 2015.
66. Kohno M and Pouyssegur J: Targeting the ERK signaling pathway in cancer therapy. Ann Med 38: 200-211, 2006.
67. Dong Z, Ma W, Huang C and Yang CS: Inhibition of tumor promoter-induced activator protein 1 activation and cell transformation by tea polyphenols, (-)-epigallocatechin gallate, and theaflavins. Cancer Res 57: 4414-4419, 1997.
68. Vivas-Mejia P, Benito JM, Fernandez A, Han H-D, Mangala L, Rodriguez-Aguayo C, Chavez-Reyes A, Lin YG, Carey MS, Nick AM, et al: JNK-1 inhibition leads to antitumor activity in ovarian cancer. Clin Cancer Res 16: 184-194, 2010.
69. Kitanaka C, Sato A and Okada M: JNK signaling in the control of the tumor-initiating capacity associated with cancer stem cells. Genes Cancer 4: 388-396, 2013.